ARTICLE OPEN

Check for updates

Flexible micro-LED display and its application in Gbps multi-channel visible light communication

Luhing Hu [1], Jaeyong Choi[1], Sumin Hwangbo[1], Do-Hoon Kwon[1], Bongkyun Jang[2], Seunghyeon Ji[1], Jae-Hyun Kim[2✉], Sang-Kook Han[1✉] and Jong-Hyun Ahn [1✉]

A flexible full-color micro-LED display with high mechanical robustness was fabricated by printing quantum dots (QDs) on a blue micro-LED array using standard photolithography. The red and green colors yielded from QDs exhibit a better color gamut than conventional color filters. The light conversion efficiency was enhanced by adding TiO_2 nanoparticles to the QD-photoresist composite. This full-color micro-LED display was successfully mounted on various unusual substrates such as curved glass, fabrics, and human skin, enabling diverse optoelectronic applications. In addition, wireless multi-channel visible light communication (VLC) based on the wavelength-division-multiplexing orthogonal-frequency-division-multiplexing (WDM-OFDM) technique was demonstrated using a QD-based color micro-LED panel. A high data transmission rate of 1.9 Gbps was successfully obtained owing to the high electrical–optical modulation bandwidth of the QD-based micro-LED panel.

INTRODUCTION

Recently, micro-light-emitting diodes (micro-LEDs) have emerged as next-generation display technology because of their superior ability to withstand moisture and provide ultrahigh luminance, and long lifespan compared to organic light-emitting diode (OLED) displays and liquid crystal displays (LCDs)[1–6]. Owing to these properties, researchers have applied micro-LEDs in smart wearable displays, automobile displays, stretchable displays, and outdoor signage[4,7–9]. In addition, micro-LEDs can be used as transmitters in VLC due to their high switching rate, high energy efficiency, and high modulation bandwidth[10,11]. They can wirelessly transmit data at high speeds. The radio frequency (RF) spectrum, the most used band in modern wireless communication systems, is already congested owing to the high demand for wireless data traffic[12]. VLC systems, which modulate the visible light spectrum to facilitate data transmission, have been investigated to replace the congested radio spectrum for wireless communication. In addition, the high bandwidth of the visible light spectrum can accommodate many users at high transmission rates for 5G communication applications[13].

Micro-LEDs have the potential to integrate displays and wireless communication systems. However, the fabrication complexity increases with the decrease in the size of LED chips, which hinders the commercialization of the products[14,15]. One of the issues in micro-LED displays is the realization of a full-color RGB display that meets the standard specifications required by modern displays[16–18]. The most widely-used method for fabricating an RGB micro-LED display is to transfer the red (R), green (G), and blue (B) micro-LED arrays from three different epitaxial wafers on the target substrate[19]. However, this approach has several challenges, such as aligning LEDs during the transfer process and electrical bonding between the LEDs and metal electrodes of display backplanes, which could raise an issue to the production yield. Although prototypes of RGB micro-LED displays have been successfully demonstrated through the transfer method, the

problem of high production costs due to low transfer yield remains a challenge[20]. Unlike traditional methods, where three different LEDs are transferred to yield an RGB display, quantum dots (QDs) have been used as a color conversion layer on a blue gallium nitride (GaN) micro-LED array[21]. These RGB LED pixels can simultaneously transmit data using different wavelengths of light, making it possible to transmit a lot of data at once. However, it is still challenging to produce an RGB micro-LED array using a QD color conversion layer on flexible substrates for VLC.

In this work, we developed a patternable QD-photoresist (PR) for photolithography. This strategy facilitates the formation of full-color micro-LED displays without complicated transfer of sub-pixels and avoids alignment issues during their assembly. We transferred a GaN-based flip-chip micro-LED array onto a flexible substrate with the micro-LED electrodes facing up. A QD color conversion layer for the red and green sub-pixels was precisely defined by photolithography to yield a flexible full-color micro-LED display. Further, the micro-LED array with QD-PR acts as the optical source for wavelength division multiplexing (WDM)-VLC and facilitates a high-speed VLC link for free-space applications using orthogonal frequency division multiplexing (OFDM). R, G, and B pixels allow for separate data transmission at different wavelengths at the same time, enabling massive data transmission that is essential for light fidelity (LiFi) communication.

RESULTS

Fabrication of flexible micro-LED display

Different lift-off methods have been developed to transfer the micro-LED array depending on the growth substrate (Fig. 1a). Chemical lift-off and laser lift-off (LLO) were used to release GaN-based micro-LED arrays from silicon and sapphire substrates, respectively. First, the micro-LED devices were formed on silicon and sapphire substrates using standard semiconductor fabrication, including photolithography, etching, chemical vapor

[1]School of Electrical and Electronic Engineering, Yonsei University, Seoul 03722, Republic of Korea. [2]Department of Nanomechanics, Nano-Convergence Mechanical Systems Research Division, Korea Institute of Machinery & Materials (KIMM) 156 Gajeongbuk-ro, Yuseong-gu, Daejeon 34103, Republic of Korea. ✉email: jaehkim@kimm.re.kr; skhan@yonsei.ac.kr; ahnj@yonsei.ac.kr
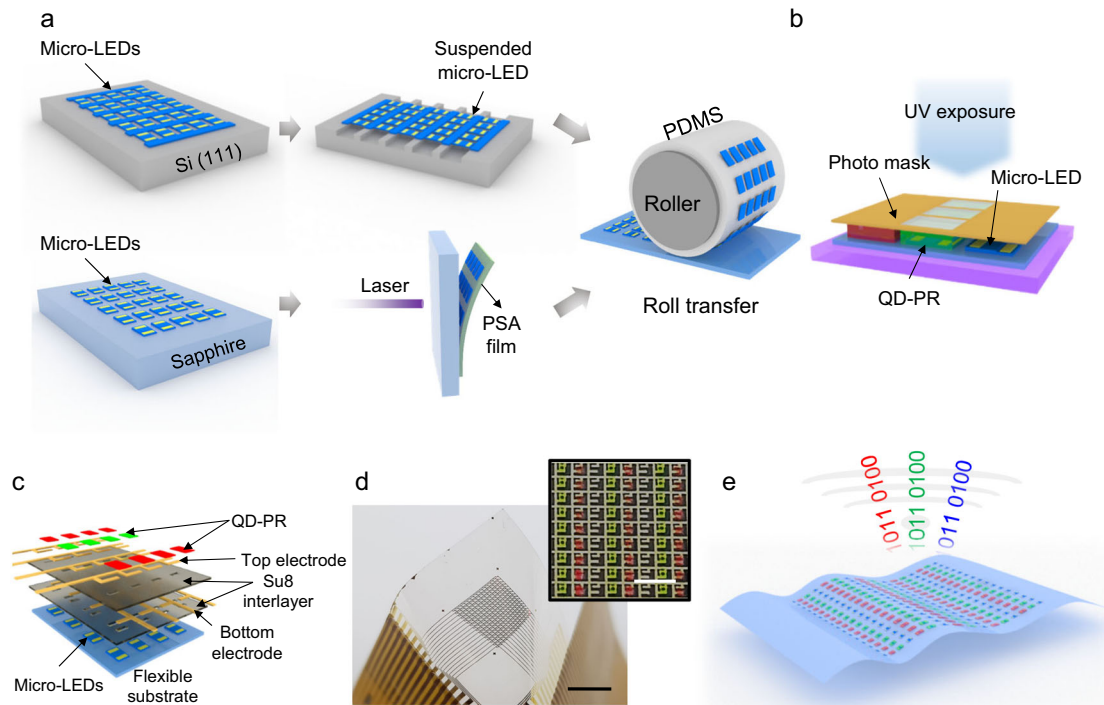
Fig. 1 QD-based flexible micro-LED display for VLC application. a Schematic of transferring a micro-LED array from mother substrate to target substrate using roll transfer. **b** Patterning of QD-PR on micro-LED array using conventional photolithography. **c** Schematic illustration of the interconnection of micro-LED display in passive matrix configuration. **d** Optical image of micro-LED display fabricated on plastics substrate and magnified image (inset) of patterned QD-PR on micro-LED display. Scale bar: 5 mm. Scale bar: 1 mm (inset). **e** Schematic shows a flexible micro-LED display and 3-channel wireless communication through the visible light spectrum.

deposition (CVD), and metal deposition. During the chemical lift-off, the underlying silicon was etched in a warm potassium hydroxide (KOH) solution to create a suspended micro-LED array, and the alignment of the array was supported using a set of anchors, which were defined by mesa[22]. The second approach to release the micro-LED devices is LLO, which offers high efficiency and high throughput over a large area with almost negligible damage to the devices[23,24]. A temporary substrate, pressure-sensitive adhesive (PSA) film, was used to hold the micro-LED array during the LLO. After the lift-off, a roll-based transfer system was used to precisely pick up the array and print it on a foreign substrate with an adhesive layer (NOA 63)[25]. A completely automated system can offer various advantages, such as high accuracy of the alignment of the micro-LED array, which facilitates the integration of the metal interconnections and a high transfer yield owing to the well-controlled applied pressure at the rubber-based roller. A QD-based color conversion layer was defined on the blue GaN micro-LEDs using the standard photolithography for a practical micro-LED application with full-color emission (Fig. 1b). This strategy has several advantages: first, the complex transfer of red and green sub-pixels can be skipped. Second, the active color conversion layer offers higher efficiency and a better color gamut of the display than conventional color filters. Third, photolithography is compatible with standard fabrication and can be applied to large-area displays. We developed a patternable QD-PR by mixing colloidal QDs in transparent negative PR (SU-8) at a specific concentration to achieve a high color conversion efficiency. After forming the interlayers and metal interconnections on the micro-LED array, the QD-PR was patterned on the desired position to yield RGB pixels (Fig. 1c). The integrated full-color micro-LED display on a 6-µm polyethylene terephthalate (PET) substrate exhibited high mechanical flexibility (Fig. 1d). The red and green QD-PRs were well defined on the micro-LED display (inset

of Fig. 1d). Finally, the data transmission using the RGB micro-LEDs was demonstrated (Fig. 1e).

Photolithographically patternable QD-PR

Figure 2 presents the development of QD-PRs. QD-PR arrays of 50 µm × 50 µm were successfully patterned on a glass substrate with a height of 10.8 ± 0.5 µm for the red and green QD-PRs (Fig. 2a, left; Fig. 2b, left; Supplementary Figs. 1, 2). Unlike passive color filters that are commonly used in current display technologies to block specific wavelengths for achieving the desired color, a QD-based active color conversion layer emits color at a specific wavelength when excited by photons[26]. Considering the absorption spectra of QD-PRs, the red and green QDs exhibit high absorption at a wavelength of 450 nm, which is the peak wavelength of the blue micro-LED device. When the QDs are excited by a photon that originates from the blue micro-LED, the QDs convert the light to red and green spectra at 630 and 530 nm, respectively (Figs. 2a, b right; Supplementary Table 1). However, blue light leakage during color conversion remains an issue. Two strategies have been investigated to resolve this issue: (1) controlling the QD concentration in the PR and (2) adding the scattering nanoparticles in the QD-PR. The color properties were investigated for different concentrations of QD-PR and nanoparticle density to achieve an optimal QD-PR. The concentration of the red QDs changed from 10 to 50 wt%. According to the electroluminescence (EL) spectra, the red peak (630 nm) increased as the concentration of the QDs in SU-8 increased, while the blue peaks almost diminished to zero. The corresponding color coordination of each concentration is plotted in a CIE diagram, as shown in Supplementary Fig. 3. To achieve a high conversion efficiency, the QDs must be well-dispersed in the PR solution without aggregation. The aggregation of QDs leads to fluorescence quenching, and the photoluminescence (PL) of the QDs
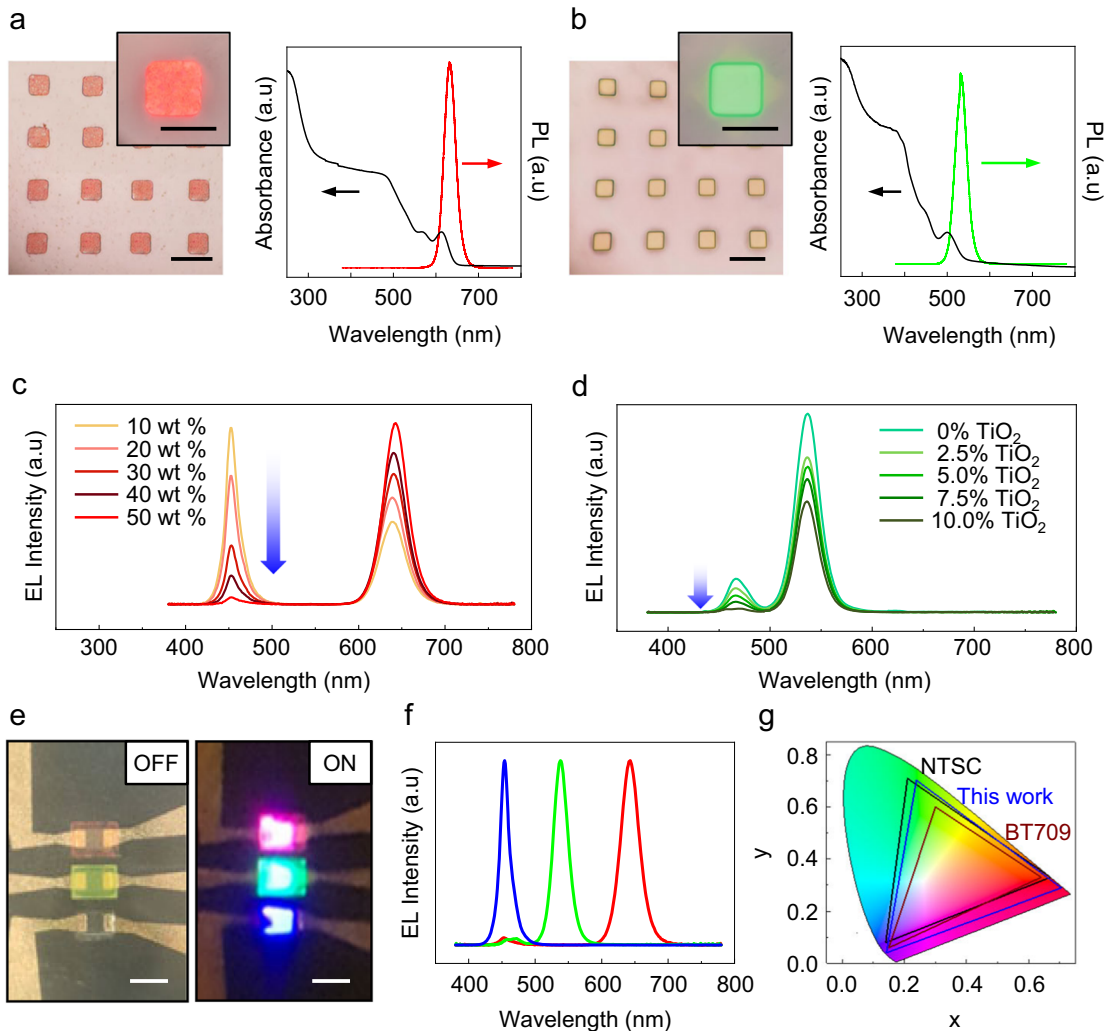
Fig. 2 Photolithographically patternable QD-PR. Optical images of patterned QD-PR, photoluminescence spectra, and UV-Vis absorption spectra of red QD (**a**) and green QD (**b**), respectively. QDs with a size of 50 μm × 50 μm are patterned on a glass substrate. Scale bar: 100 μm. Scale bar: 50 μm (inset). **c** Electroluminescence spectra of the micro-LED coated with red QD-PR are measured by varying the concentration of QDs in PR (10, 20, 30, 40, and 50 wt%). **d** Electroluminescence spectra of the micro-LEDs after mixing TiO₂ into 30 wt% green QD-PR (0, 2.5, 5, 7.5, and 10%). **e** Optical image showing the off state (left) of the micro-LEDs with patterned QD-PR and on-state (right) after the application of forward voltage. Scale bar: 200 μm. Electroluminescence spectra (**f**) and CIE chromaticity (**g**) indicating the color properties of the fabricated RGB micro-LEDs.

significantly decreases[27]. Therefore, before mixing with the PR solution, the QDs are dispersed in cyclopentanone through ultrasonication to prevent aggregation. The light conversion efficiency (*LCE*) is calculated using the formula: $LCE = \frac{I_{QD}}{I_{Blue} - I_{Blue,Leak}}$, where, I_{QD} is the light intensity after the QD conversion, I_{Blue} denotes the blue light from the GaN micro-LED chip, and $I_{blue,Leak}$ is the blue peak after the QD conversion. The *LCE* of the red QD-PR was 36% at a concentration of 50 wt%. However, a high concentration of QD in PR solution can hinder the development of the PR film, and polymer residues can remain on the substrate after the process. This issue can be resolved by blending the scattering nanoparticles into the QD-PR solution[28]. TiO₂ nanoparticles exhibit a high refractive index of 2.8 and can be utilized as scattering enhancers in the QD color conversion layers. With the addition of TiO₂ nanoparticles, the blue light absorption of the QDs can be enhanced as more light is transferred to the QDs. The emitted light of QDs increases at the peak wavelength through photoluminescence because the total internal reflection is avoided due to the scattering effect of the nanoparticles. We fixed the concentration of the green QDs at 30 wt% and mixed the

TiO₂ nanoparticles from 0 to 10 wt%. The resulting EL spectra and their corresponding color coordination are shown in Fig. 2d and Supplementary Fig. 4, respectively. The *LCE* was 43% for 10 wt% TiO₂ in the QD-PR.

For demonstrating the versatility of the QD-PRs, the red and green QD-PRs were defined on the LEDs to form RGB pixels (Fig. 2e). Three distinct colors (red, green, and blue) were clearly visible when the LEDs were turned on. The corresponding normalized EL spectra are shown in Fig. 2F. In addition, the color gamut of the RGB pixels was measured and plotted on the CIE 1976 chromaticity diagram (Fig. 2f). Notably, the QD-PRs exhibited a larger coverage area on the CIE diagram than the NTSC and BT709, which are the standard for modern ultra-high definition (UHD) displays (Supplementary Table 2).

Flexible full-color micro-LED display
We developed a prototype of full-color micro-LED display by patterning the optimized QD-PRs on a large-area micro-LED array (20 × 20 pixels) after the metal interconnection process (Supplementary Fig. 5). The fabrication was performed on a 6-μm thick PET
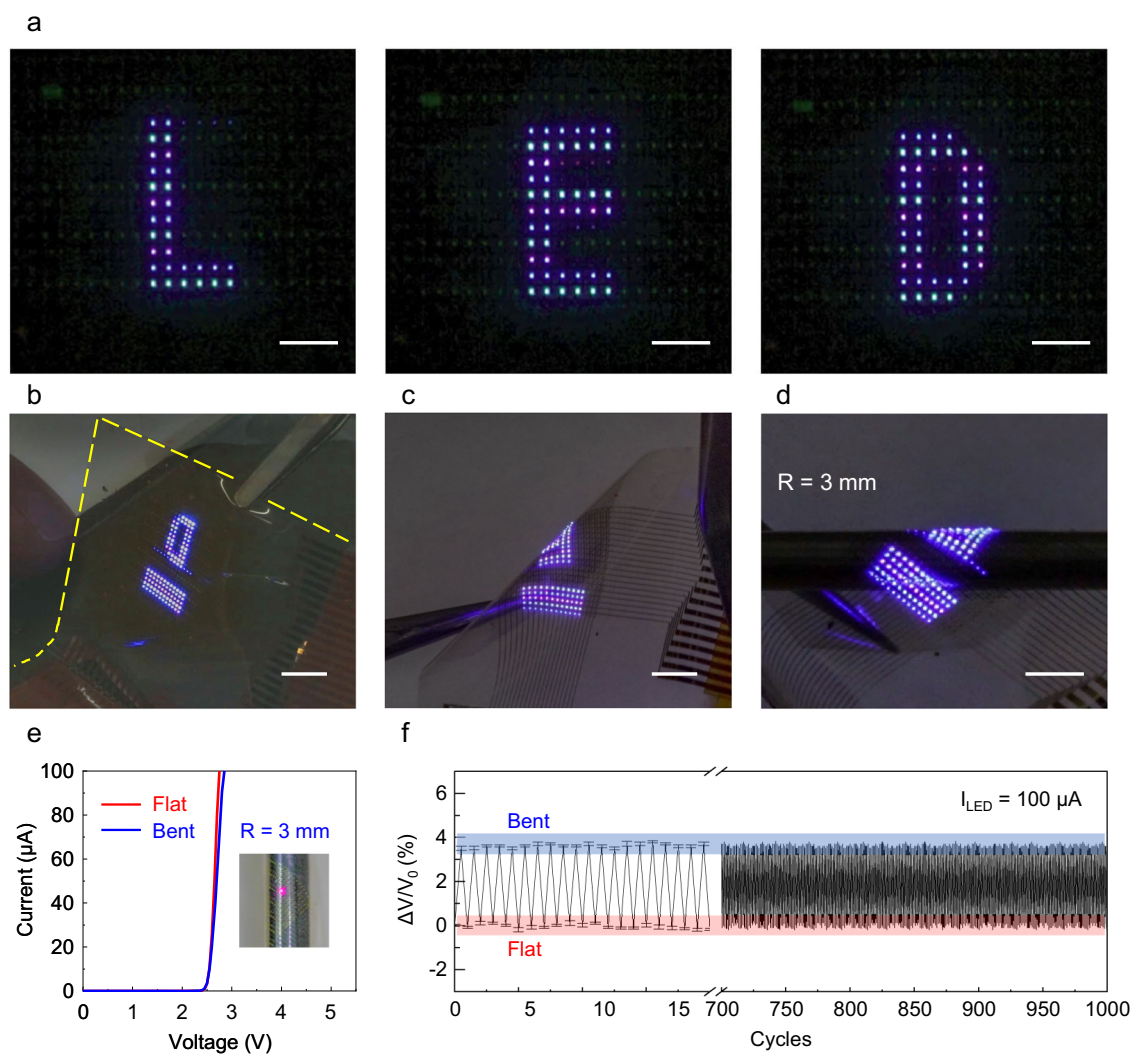
Fig. 3 Flexible full-color micro-LED display. a Optical images of the dynamic operation of micro-LED display using external driving circuit, representing the letters 'L,' 'E,' and 'D'. Scale bar: 2 mm. **b** Optical image of full-color micro-LED display after peeling off from the carrier substrate. Scale bar: 5 mm. **c** Optical image of RGB micro-LED display, when bent by tweezers. Scale bar: 5 mm. **d** Photograph of ultrathin RGB micro-LED display on a glass rod with 3 mm radius. Scale bar: 6 mm. **e** Current–voltage curves of micro-LEDs, when bent with R = 3 mm. **f** Relative voltage change of micro-LED during cyclic bending test with a bending radius of 3 mm. The injected current during the test is fixed at 100 µA.

substrate, which provides low mechanical stiffness. Further, the fabricated display was connected to an external driving circuit via a flexible printed circuit board (FPCB) for display operations (Supplementary Fig. 6, Supplementary Fig. 7). Moreover, an additional graphene heat spreading layer can be inserted between the micro-LED array and the plastic substrate for better heat dissipation. Graphene distributes the central temperature of micro-LED heating evenly on a two-dimensional plane to facilitate uniform heat dissipation (Supplementary Fig. 8)[29]. The letters 'L,' 'E,' and 'D' were encoded to the display driving unit and presented on the micro-LED display through line addressing (Fig. 3a; Supplementary Movie 1). The full-color display operated stably without mechanical failure owing to its low bending stiffness when peeled off from the glass handling substrate and bent by a tweezer (Fig. 3b, c; Supplementary Movie 2). To further validate the mechanical robustness of the micro-LED display, cyclic bending tests were performed. No significant change in the luminance of the display was observed when it was bent and rolled on a rod with a bending radius of 3 mm (Fig. 3d; Supplementary Movie 3). In addition, the electrical properties of the micro-LEDs were investigated during the cyclic bending test (Fig. 3e). The variation

in the operating voltage was less than ~4.5% after 1000 bending cycles under operating current of 100 µA (Fig. 3f). The change in operating voltage could be recovered when the display was flattened. In addition, the change in the luminance of the micro-LEDs and EL peak is negligible after the cyclic bending test under currents of 100 µA, 500 µA, and 1 mA (Supplementary Fig. 9). Therefore, we can conclude that the slight variation in electrical properties and mechanical bending did not affect the performance of the micro-LED display. The high mechanical flexibility could be attributed to the low bending stiffness of the display substrate and the isolation of each micro-LED pixel.

The good mechanical feature of the micro-LED display allows it to attach to various types of unusual surfaces, such as thin glass, fabric, and human skin, and provide invariant properties even under deformation. A 3 µm-thick double-sided adhesive layer was utilized to give the display the ability to perform like a sticker that can attach on target surfaces. As a demonstration, the ultrathin display was attached to a curved glass with a bending radius of 4 cm (Fig. 4a). Recently, augmented reality (AR)-embedded head-up displays have grabbed much attention as the next-generation displays for automobiles. Micro-LED displays promise to deliver
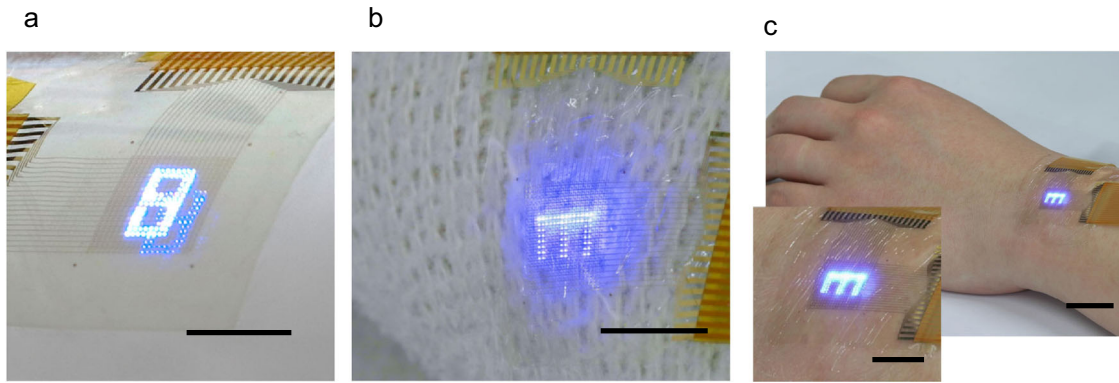
Fig. 4 Micro-LED array for sticker-like ultrathin display on various substrates. a Optical image of micro-LED display on a curve glass with a bending radius of 4 cm. Scale bar: 1 cm. **b** Image of the ultrathin display on a knit fabric. Scale bar: 1 cm. **c** Optical images of micro-LED display mounted on human skin. Scale bar: 2 cm. The inset provides a magnified view of the display in operation showing alphabet 'E'. Scale bar: 1 cm.

multiple advantages for automobile displays over conventional OLED displays, such as high brightness, better reliability against moisture and high temperatures, and low power consumption. The flexible sticker-like micro-LED display offers a strategy to integrate the displays on vehicles by simply attaching the display on curved windshields. A wearable display is another prominent application as it can effectively deliver the output information to the users[30]. We attached the flexible micro-LED display on a knitted fabric to produce a wearable display (Fig. 4b). A wearable micro-LED display integrated with LiFi applications is a promising approach to let users interact with the Internet of Things (IoT), in which the physical objects are connected to the digital network. In addition, Fig. 4c shows the operation of this sticker-like micro-LED display on a soft surface like human skin. A conformal contact of the electronics systems and the human skin surface is strongly dependent on the mechanical properties of the device including, Young's modulus, thickness, stiffness, adhesion, and the Poisson's ratio of each layout in the display system[31,32]. To achieve flawless contact with the skin, the micro-LED display was fabricated by integrating materials with low stiffness that can adhere to the wrinkles of the skin surfaces. The low bending stiffness of the ultrathin micro-LED display allows the system to perform with minimum degradation in both luminance and electrical properties due to deformations induced by human skin. As a result, the ultrathin micro-LED display is conformally mounted on the human skin and operates robustly without failure.

Wireless VLC based on QD-based micro-LED array

Micro-LEDs exhibit a high electrical–optical modulation bandwidth, making them a suitable optical source for VLC applications. We demonstrated high-speed data transmission using QD-based color micro-LEDs enabled by the QD-PRs through the WDM-OFDM scheme. The OFDM is a kind of digital multi-carrier scheme in which the bandwidth of an optical source is completely utilized to encode digital data on multiple subcarriers[33]. To realize the 3–channel RGB communication link, WDM-VLCs that enabled the data to be individually carried by the three wavelengths of the RGB micro-LEDs were implemented. Figure 5a shows the experimental setup of the communication link that consisted of the micro-LEDs with the QD-PRs as the optical sources and a commercial avalanche photodiode (APD) as the receiver. The VLC is performed wirelessly in a free-space of 30 cm. The OFDM signals were generated using an arbitrary waveform generator (AWG) after MATLAB coding, and the signals at the receiver end were received by an oscilloscope and processed in MATLAB, including fast Fourier transform and demodulation. For the high throughput of the WDM VLC link, dichroic filters were

placed in front of the APD to prevent optical crosstalk between the wavelengths. The frequency response of the GaN blue micro-LED was from 5 to 250 MHz, indicating that the system is above the noise level. Therefore, it can be completely utilized by the OFDM scheme and can provide a large bandwidth for data transmission (Fig. 5b, Supplementary Fig. 10). We implemented the OFDM signals that contained 256 subcarriers to occupy the bandwidth of the system. The bit allocation on each subcarrier is shown in Fig. 5c, which correlates with the achieved SNR values in Fig. 5d. Notably, the red and green channels enabled by the QD-PR exhibit fewer allocated bits than the blue channel because the long fluorescence lifetime of the QDs limits the optical bandwidth of the channel[34]. However, it is noteworthy that the QD-based color conversion layer exhibits shorter fluorescent lifetime than that of phosphor-based color filter, which provide not only better color purity, but also improve the modulation bandwidth[35]. The BER for each subcarrier is shown in Fig. 5e. The total BER of the link was 5.41×10^{-4}, which is below the forward error correction (FEC) target (2×10^{-3}). As a result, the blue channel showed the highest data rate of 964 Mbps, while the red and green channels exhibited the data rates of 529 and 460 Mbps, respectively. Hence, a total of 1.9 Gbps data transmission was achieved when the optical filters were used at the receiver to allow the desired wavelength to be processed in the WDM VLC link (Supplementary Table 3).

DISCUSSION

We successfully fabricated a flexible full-color micro-LED display with high mechanical flexibility using QD-PR as the color conversion layer on an array of GaN micro-LEDs. The fabrication of the flexible micro-LED display through the roll-transfer method provides high accuracy in the alignment of the LEDs and high productivity while preserving the performances of the devices during the process. In addition, the QD-based color conversion layers enable display size scalability as they can be defined via a foundry-compatible photolithography process. The developed QD-based color micro-LED application in an OFDM-based WDM VLC system was analyzed, and a high data transmission rate of 1.9 Gbps was achieved. The outstanding electrical-optical modulation properties of the micro-LEDs enable Gbps multi-channel VLC, which is difficult to be achieved by conventional light sources. A combination of flexible micro-LED display and wireless data transmission may accelerate the development of next-generation technologies, such as the IoT, LiFi, and intelligent wearable electronics.
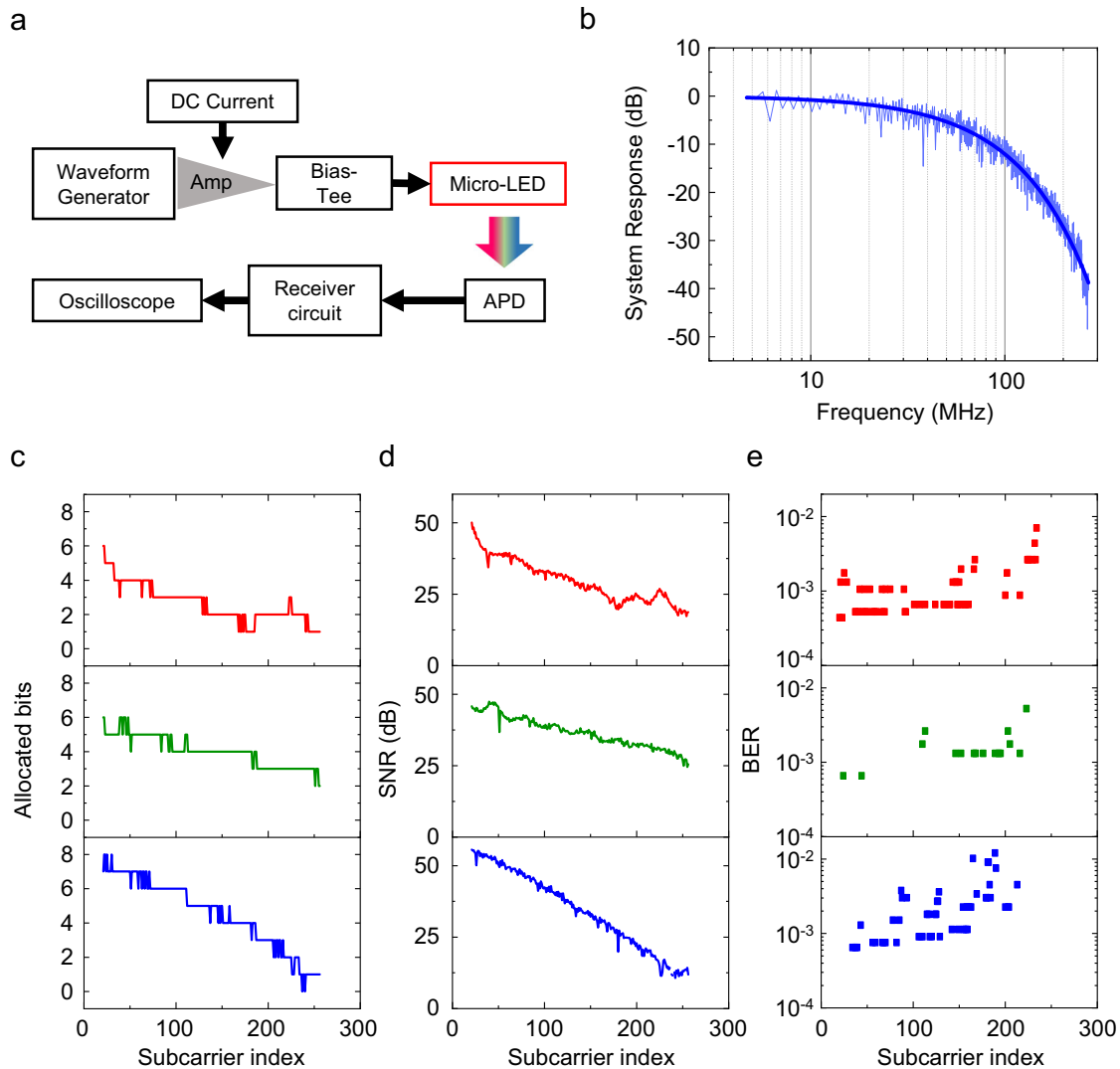
Fig. 5 OFDM-based WDM VLC application. a Flow chart of the experimental setup for 3-channel wireless visible light communication. **b** Frequency response of the blue micro-LED. **c** The adaptive bit loading for each subcarrier. Graphs showing the measured SNR (**d**) and BER (**e**) at different frequency subcarrier.

METHODS

Fabrication of micro-LEDs

GaN was epitaxially grown on silicon and sapphire wafers. n-GaN was etched by inductively coupled plasma-reactive ion etching (ICP-RIE) using BCl_3 and N_2 plasma. To form an n-type ohmic contact, metal layers (Cr/Au: 3/50 nm) were deposited and annealed at 300 °C under a N_2 atmosphere. Next, p-type ohmic contacts (Ni/Au: 10/50 nm) were defined on p-GaN. A 100-nm thick silicon nitride passivation layer was deposited using plasma-enhanced chemical vapor deposition (PECVD). An etch mask (PR 4620) was generated to define the geometry of the micro-LEDs, and the exposed regions were etched using ICP-RIE. Further, the micro-LED array was released from the substrate either using a chemical or laser-assisted method. An adhesive layer (NOA 63) was spin-coated onto a thin PET substrate, which was attached to a handling substrate with a layer of polydimethylsiloxane (PDMS). The micro-LED array was then printed on the target substrate using an automated roll transfer system.

Preparation of QD-PR

CdSe/ZnS core-shell QDs (Fine Lab) are used. The QD/toluene solution was stirred using a magnetic bar to evaporate the solvent at room temperature. Further, the QDs were dispersed in SU-8 Thinner (MicroChem) in an ultrasonic bath. After confirming the absence of the aggregation of the QDs, a transparent negative photoresist, SU-8 2015 (MicroChem), was added to the solution and stirred at 150 rpm overnight in an ambient environment.

Photoluminescence and electroluminescence measurement

The PL of the QDs was obtained using a Raman spectrometer (Horiba, LabRAM ARAMIS) with an external laser source of 325 nm. The EL characteristics of the micro-LEDs with QD-PRs were obtained using a spectroradiometer (Konica Minolta, CS2000) with Keithley 2635A source meter.

VLC link

The OFDM signals are generated using an AWG (Tektronix, AWG7002A). These signals were DC-biased with a bias-tee (Mini-Circuits, ZFSCJ-2-2-S) and fed to the micro-LEDs. At the receiver, an APD (Hamamatsu, C5331-11) detected the optical signal and analyzed them using a digital oscilloscope (Tektronix, MSO71604C). The signals were processed offline through MATLAB.

DATA AVAILABILITY

The data that support the plots within these paper and other findings of this study are available from the corresponding authors upon reasonable request.

REFERENCES

1. Huang, Y., Hsiang, E.-L., Deng, M.-Y. & Wu, S.-T. Mini-LED, Micro-LED and OLED displays: present status and future perspectives. *Light Sci. Appl.* **9**, 105 (2020).
2. Park, S.-I. et al. Printed assemblies of inorganic light-emitting diodes for deformable and semitransparent displays. *Science* **325**, 977–981 (2009).
3. Pust, P., Schmidt, P. J. & Schnick, W. A revolution in lighting. *Nat. Mater.* **14**, 454–458 (2015).
4. Wu, T. et al. Mini-LED and micro-LED: promising candidates for the next generation display technology. *Appl. Sci.* **8**, 1557 (2018).
5. Zhang, H. & Rogers, J. A. Recent advances in flexible inorganic light emitting diodes: from materials design to integrated optoelectronic platforms. *Adv. Opt. Mater.* **7**, 1800936 (2019).
6. Hwangbo, S. et al. Wafer-scale monolithic integration of full-colour micro-LED display using MoS₂ transistor. *Nat. Nanotechnol.* **17**, 500–506 (2022).
7. Lee, V. W., Twu, N. & Kymissis, I. Micro-LED technologies and applications. *J. Inf. Disp.* **32**, 16–23 (2016).
8. Lee, Y. et al. Morphable 3D structure for stretchable display. *Mater. Today* **53**, 51–57 (2022).
9. Jang, B. et al. Auxetic meta-display: stretchable display without image distortion. *Adv. Funct. Mater.* **32**, 2113299 (2022).
10. Islim, M. S. et al. Towards 10 Gb/s orthogonal frequency division multiplexing-based visible light communication using a GaN violet micro-LED. *Photon. Res.* **5**, A35–A43 (2017).
11. Tsonev, D. et al. A 3-Gb/s single-LED OFDM-based wireless VLC link using a gallium nitride µLED. *IEEE Photon. Technol. Lett.* **26**, 637–640 (2014).
12. Karunatilaka, D., Zafar, F., Kalavally, V. & Parthiban, R. LED based indoor visible light communications: state of the art. *IEEE Commun. Surv. Tutor.* **17**, 1649–1678 (2015).
13. Feng, L. et al. Applying VLC in 5G networks: architectures and key technologies. *IEEE Netw.* **30**, 77–83 (2016).
14. Park, J. et al. Electrically driven mid-submicrometre pixelation of InGaN micro-light-emitting diode displays for augmented-reality glasses. *Nat. Photon.* **15**, 449–455 (2021).
15. Kim, R.-H. et al. Waterproof AlInGaP optoelectronics on stretchable substrates with applications in biomedicine and robotics. *Nat. Mater.* **9**, 929–937 (2010).
16. Choi, M. et al. Full-color active-matrix organic light-emitting diode display on human skin based on a large-area MoS₂ backplane. *Sci. Adv.* **6**, eabb5898 (2020).
17. Han, H.-V. et al. Resonant-enhanced full-color emission of quantum-dot-based micro LED display technology. *Opt. Express* **23**, 32504–32515 (2015).
18. Yin, Y. et al. Full-color micro-LED display with CsPbBr₃ perovskite and CdSe quantum dots as color conversion layers. *Adv. Mater. Technol.* **5**, 2000251 (2020).
19. Bower, C. A. et al. Emissive displays with transfer-printed assemblies of 8 µm× 15 µm inorganic light-emitting diodes. *Photon. Res.* **5**, A23–A29 (2017).
20. Anwar, A. R. et al. Recent progress in micro-LED-based display technologies. *Laser Photon. Rev.* **16**, 2100427 (2022).
21. Kim, H.-M. et al. Ten micrometer pixel, quantum dots color conversion layer for high resolution and full color active matrix micro-LED display. *J. Soc. Inf. Disp.* **27**, 347–353 (2019).
22. Kim, H.-S. et al. Unusual strategies for using indium gallium nitride grown on silicon (111) for solid-state lighting. *Proc. Natl Acad. Sci. USA* **108**, 10072–10077 (2011).
23. Bian, J. et al. Laser transfer, printing, and assembly techniques for flexible electronics. *Adv. Electron. Mater.* **5**, 1800900 (2019).
24. Kim, J., Kim, J.-H., Cho, S.-H. & Whang, K.-H. Selective lift-off of GaN light-emitting diode from a sapphire substrate using 266-nm diode-pumped solid-state laser irradiation. *Appl. Phys. A* **122**, 305 (2016).
25. Choi, M. et al. Stretchable active matrix inorganic light-emitting diode display enabled by overlay-aligned roll-transfer printing. *Adv. Funct. Mater.* **27**, 1606005 (2017).
26. Kim, H.-J., Shin, M.-H. & Kim, Y.-J. Optical efficiency enhancement in white organic light-emitting diode display with high color gamut using patterned quantum dot film and long pass filter. *Jpn. J. Appl. Phys.* **55**, 08RF01 (2016).
27. Noh, M. et al. Fluorescence quenching caused by aggregation of water-soluble CdSe quantum dots. *Colloids Surf. A Physicochem. Eng. Asp.* **359**, 39–44 (2010).
28. Kim, Y.-J. et al. 52.2: Invited Paper: application of quantum-dot patterned film with scattering nanoparticles for the high efficiency displays. *SID Symp. Dig. Tech. Pap.* **50**, 572–574 (2019).
29. Bae, S. H. et al. Graphene-based heat spreader for flexible electronic devices. *IEEE Trans. Electron Devices* **61**, 4171–4175 (2014).
30. Lee, H. E. et al. Wireless powered wearable micro light-emitting diodes. *Nano Energy* **55**, 454–462 (2019).
31. Kim, J. et al. 2D Materials for skin-mountable electronic devices. *Adv. Mater.* **33**, 2005858 (2021).
32. Liu, S. et al. Strategies for body-conformable electronics. *Matter* **5**, 1104–1136 (2022).
33. Xie, E. et al. Over 10 Gbps VLC for long-distance applications using a GaN-based series-biased micro-LED array. *IEEE Photon. Technol. Lett.* **32**, 499–502 (2020).
34. Mei, S. et al. High-bandwidth white-light system combining a micro-LED with perovskite quantum dots for visible light communication. *ACS Appl. Mater. Interfaces* **10**, 5641–5648 (2018).
35. Xiao, X. et al. Improving the modulation bandwidth of LED by CdSe/ZnS quantum dots for visible light communication. *Opt. Express* **24**, 21577–21586 (2016).

AUTHOR CONTRIBUTIONS

J.-H.A. planned and supervised the project. L.H. conducted most of the experiments regarding the device fabrication and characterized the properties of the devices. J.C., S.H., and S.J. supported the experiments. J.-H.K. and B.J. helped to transfer the micro-LEDs. S.-K.H. and D.-H.K. investigated the VLC link. All authors analyzed the data and wrote the manuscript.

COMPETING INTERESTS

The authors declare no competing interests.

ADDITIONAL INFORMATION

Supplementary information The online version contains supplementary material available at https://doi.org/10.1038/s41528-022-00234-z.

Correspondence and requests for materials should be addressed to Jae-Hyun Kim, Sang-Kook Han or Jong-Hyun Ahn.

Reprints and permission information is available at http://www.nature.com/reprints

Publisher's note Springer Nature remains neutral with regard to jurisdictional claims in published maps and institutional affiliations.